Inorganic Chemistry

Article

pubs.acs.org/IC

Synthesis, Structural, and Magnetic Characterization of Linear and Bent Geometry Cobalt(II) and Nickel(II) Amido Complexes: Evidence of Very Large Spin−Orbit Coupling Effects in Rigorously Linear Coordinated Co^{2+}

Aimee M. Bryan,[†] W. Alexander Merrill,[†] William M. Reiff,[‡,§] James C. Fettinger,[†] and Philip P. Power*[,†]

[†]Department of Chemistry, University of California, Davis, One Shields Avenue, Davis, California 95616, United States

[‡]Department of Chemistry and Chemical Biology, Northeastern University, Boston, Massachusetts 02115, United States

[§]National High Magnetic Field Laboratory, Florida State University, Tallahassee, Florida 32310, United States

Supporting Information

ABSTRACT: The complexes M(II){N(H)$Ar^{Pr^i_6}$}$_2$ (M = Co, **1** or Ni, **2**; $Ar^{Pr^i_6}$ = C_6H_3-2,6(C_6H_2-2,4,6-Pr^i_3)$_2$), which have rigorously linear, N−M−N = 180°, metal coordination, and M(II){N(H)Ar^{Me_6}}$_2$ (M = Co, **3** or Ni, **4**; Ar^{Me_6} = C_6H_3-2,6(C_6H_2-2,4,6-Me_3)$_2$), which have bent, N−Co−N = 144.1(4)°, and N−Ni−N = 154.60(14)°, metal coordination, were synthesized and characterized to study the effects of the metal coordination geometries on their magnetic properties. The magnetometry studies show that the linear cobalt(II) species **1** has a very high ambient temperature moment of about 6.2 μ_B (cf. spin only value = 3.87 μ_B) whereas the bent cobalt species **3** had a lower μ_B value of about 4.7 μ_B. In contrast, both the linear and the bent nickel complexes **2** and **4** have magnetic moments near 3.0 μ_B at ambient temperatures, which is close to the spin only value of 2.83 μ_B. The studies suggest that in the linear cobalt species **1** there is a very strong enhanced spin orbital coupling which leads to magnetic moments that broach the free ion value of 6.63 μ_B probably as a result of the relatively weak ligand field and its rigorously linear coordination. For the linear nickel species **2**, however, the expected strong first order orbital angular momentum contribution does not occur (cf. free ion value 5.6 μ_B) possibly because of π bonding effects involving the nitrogen p orbitals and the d_{xz} and d_{yz} orbitals (whose degeneracy is lifted in the C_{2h} local symmetry of the Ni{N(H)C(*ipso*)}$_2$ array) which quench the orbital angular momentum.

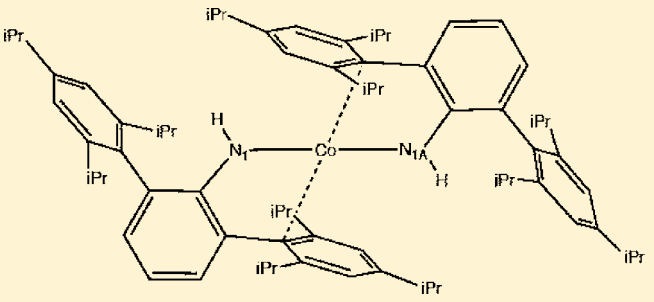

INTRODUCTION

For open-shell (d^1-d^9) transition metal complexes those having two-coordinate metals are among the least studied.[1,2] Of the stable two-coordinate complexes currently known most (ca. 80%) feature a nonlinear metal coordination in the solid state. This is caused, at least in part, by the tendency of the coordinatively unsaturated metal to display secondary interactions to other parts of the sterically large ligands that are used to maintain the low-coordination number. Strictly linear coordination is generally observed in crystalline samples only with use of the bulkiest ligands. These can enforce linear coordination by steric interference between the ligands across the metal. Linear coordination is a desirable characteristic because, for some metal ions, it can permit observation of essentially free ion magnetism with a strong, unquenched, first order orbital angular momentum contribution as seen in the Fe^{2+} complexes Fe{$C(SiMe_3)_3$}$_2$[3] and Fe(NBu^t_2)$_2$.[4] Furthermore, magnetic studies of the linear and bent primary amido iron complexes Fe{N(H)$Ar^{Pr^i_6}$}$_2$ ($Ar^{Pr^i_6}$ = C_6H_3-2,6(C_6H_2-2,4,6-Pr^i_3)$_2$; N−Fe−N = 180°) and Fe{N(H)Ar^{Me_6}}$_2$ (Ar^{Me_6} = C_6H_3-2,6(C_6H_2-2,4,6-Me_3)$_2$; N−Fe−N = 140.94(16)°), featuring closely related ligands, showed that bending the geometry quenched a large portion of the first order orbital angular momentum and reduced the magnetic moment from 7.0−7.5 μ_B to 5.25−5.80 μ_B.[5] Inspection of simple d-orbital splitting diagrams of the first row transition metal M^{2+} ions in linear coordination show that first order orbital angular momentum is expected only for those that have a degenerate ground state d^1 (Sc^{2+}), d^3 (V^{2+}), d^6 (Fe^{2+}), and d^8 (Ni^{2+}) ions (Figure 1). Of these four configurations the effects of bending the geometry have been investigated only for the d^6 amido complexes of Fe^{2+} (see above). In this paper we report the synthesis and characterization of the late transition metal d^7, Co^{2+} linear and bent geometry primary amido complexes Co{N(H)$Ar^{Pr^i_6}$}$_2$ and Co{N(H)Ar^{Me_6}}$_2$ which are analogous to the corresponding iron species discussed above but for which no first order orbital angular momentum is predicted (cf. Figure 1). In addition, we describe their d^8, Ni^{2+} analogues Ni{N(H)Ar^{Pri}_6}$_2$ and Ni{N(H)Ar^{Me}_6}$_2$,

Received: June 9, 2011
Published: February 24, 2012

   dx.doi.org/10.1021/ic2012414 | *Inorg. Chem.* 2012, 51, 3366−3373

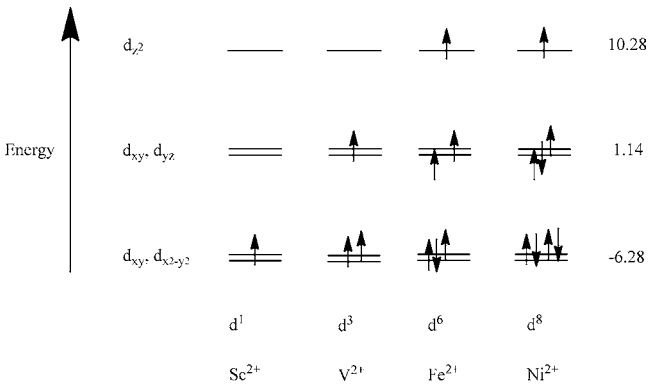

Figure 1. Splittings of the d-orbitals of the first row M^{2+} ions which are expected to display a 1st order orbital angular momentum contribution to the magnetic moment in linear, two-coordinate ligand fields. The numbers refer to *D*q values.[6]

for which first order orbital angular momentum is possible, and discuss the results of magnetic studies of these four complexes.

EXPERIMENTAL SECTION

General Procedures. All manipulations were performed with the use of modified Schlenk techniques or in a Vacuum Atmospheres drybox under N_2 or argon. Solvents were dried and collected using a Grubbs-type solvent purification system[7] (Glass Contour) and degassed by sparging with dry N_2 or Ar for 10 min or by using the freeze, pump, thaw method. All physical measurements were obtained under strictly anaerobic and anhydrous conditions. IR spectra were recorded as Nujol mulls between CsI plates on a Perkin-Elmer 1430 spectrophotometer. UV−visible spectra were recorded as dilute hexane solutions in 3.5 mL quartz cuvettes using either a HR 2000 CG-UVNIR spectrometer with Ocean Optics DH 2000 light sources on a HP 8452 diode array spectrophotometer. Melting points were determined on a Meltemp II apparatus using glass capillaries sealed with vacuum grease, and are uncorrected. Unless otherwise stated, all materials were obtained from commercial sources and used as received. $Ar^{Me_6}NH_2$,[8] and $Ar^{Pr^i_6}NH_2$[9] and $NiBr_2$(DME) (DME = 1,2-dimethoxyethane)[10] were prepared according to literature procedures.

$Co\{N(H)Ar^{Pr^i_6}\}_2$ (1). To a solution of $Ar^{Pr^i_6}NH_2$ (0.96 g, 1.9 mmol) in ca. 40 mL of Et_2O was added $LiBu^n$ (2.5 M in C_6H_{14}) (0.85 mL, 2.1 mmol) at 0 °C. After 2 h, the pale yellow solution was added dropwise to a stirred suspension of $CoCl_2$ (0.125 g, 0.96 mmol) in Et_2O (ca. 20 mL) cooled to about −78 °C. As the mixture warmed, it developed a purple color and the mixture was stirred at ambient temperature overnight. The solvent was removed under reduced pressure, and the violet solids were extracted with hexanes (ca. 40 mL). The solution was filtered through Celite and washed with hexanes (ca. 90 mL). The filtrate was concentrated to about 20 mL and stored at about −18 °C for 2 days which afforded **1** violet plates. Yield 0.770 g (76%) in two crops, mp 178 °C. Anal. Calcd. for **1**: C, 82.16; H, 9.58; N, 2.66. Found: C, 81.89; H, 9.76, N, 2.51.UV−vis, nm (ε, M^{-1} cm^{-1}) 364(sh) (1550), 566(s,br) (4350). IR, cm^{-1}: 3480, 3380, 3320 ν(N−H), 480, 380 ν(Co−N).

$Ni\{N(H)Ar^{Pr^i_6}\}_2$ (2). To a solution of $Ar^{Pr^i_6}NH_2$ (1.025 g, 2.0 mmol) in about 40 mL of Et_2O was added $LiBu^n$ (2.5 M in C_6H_{14}) (0.9 mL, 2.2 mmol) at about 0 °C. After 2 h, the pale yellow solution was added dropwise to a stirred solution of $NiBr_2$(DME) (0.227 g, 0.1 mmol) in Et_2O (ca. 40 mL) at about 0 °C. A deep blue solution resulted. After stirring at ambient temperature overnight, the solvent was removed under reduced pressure. The blue solid residue was extracted with hexane (ca. 50 mL). The solution was filtered through a Celite pad which was washed with hexane (ca. 30 mL). The deep blue filtrate was concentrated to about 25 mL and stored at about −18 °C for 2 d to give **2** as small blue, needle-shaped crystals. Yield 0.293 g (27%), mp 277 °C. Anal. Calcd. for **2**: C, 82.16; H, 9.58; N, 2.66. Found: C, 82.13; H, 10.46; N, 2.44. UV−vis, nm (ε, M^{-1} cm^{-1}) 770(s,br) (9450). IR, cm^{-1}: 3480, 3380, 3320 ν(N−H), 400 ν(Ni−N).

$Co\{N(H)Ar^{Me_6}\}_2$ (3). To a solution of $Ar^{Me_6}NH_2$ (0.723 g, 2.2 mmol) in about 30 mL of Et_2O was added $LiBu^n$ (2.5 M in C_6H_{14}) (0.97 mL, 2.4 mmol) at about 0 °C. After 2 h, this suspension was added to a stirred suspension of $CoCl_2$ (0.143 g, 1.1 mmol) in Et_2O (ca. 25 mL) at about 0 °C. The solution was allowed to warm to room temperature to give a dark violet color. The solvent was removed under reduced pressure, and the residue was extracted with toluene (ca. 25 mL) with stirring. The mixture was filtered over Celite, which was washed with about 10 mL of toluene. The filtrate was

Table 1. Selected Crystallographic and Data Collection Parameters for the Linear and Bent Complexes 1−4

	$Co\{N(H)Ar^{Pr^i_6}\}_2$ (1)	$Ni\{N(H)Ar^{Pr^i_6}\}_2$ (2)	$Co\{N(H)Ar^{Me_6}\}_2$ (3)	$Ni\{N(H)Ar^{Me_6}\}_2$ (4)
formula	$C_{72}H_{100}N_2Co$	$C_{72}H_{100}N_2Ni$	$C_{48}H_{52}N_2Co$	$C_{48}H_{52}N_2Ni$
Fw	1052.47	1052.24	715.85	715.62
color, habit	violet, plate	blue, needle	violet, block	blue, rod
crystal system	triclinic	triclinic	triclinic	triclinic
space group	$P\bar{1}$	$P\bar{1}$	$P\bar{1}$	$P\bar{1}$
a, Å	10.7214(9)	10.7334(18)	9.6706(13)	9.768(2)
b, Å	11.6119(9)	11.5751(19)	11.7687(16)	11.715(3)
c, Å	14.7576(12)	14.771(3)	18.198(3)	18.184(4)
α, deg	67.272(2)	66.827(2)	107.353(2)	108.132(3)
β, deg	73.444(2)	73.513(2)	100.442(2)	100.254(3)
γ, deg	75.880(2)	75.750(2)	95.132(2)	95.229(4)
V, $Å^3$	1605.6(2)	1598.8(5)	1921.2(5)	1921.9(7)
Z	1	1	2	2
crystal dims, mm	0.32 × 0.27 × 0.08	0.46 × 0.31 × 0.13	0.46 × 0.12 × 0.10	0.45 × 0.34 × 0.28
T, K	90(2)	90(2)	90(2)	90(2)
d_{calc}, g/cm^3	1.088	1.093	1.234	1.233
abs. coefficient μ, mm^{-1}	0.308	0.344	0.482	0.540
θ range, deg	2.00 to 25.00	2.77 to 27.47	1.20 to 27.54	2.50 to 25.09
R(int)	0.0258	0.0285	0.0217	0.0285
obs reflections [$I > 2\sigma(I)$]	5031	5714	6173	5198
data/restraints/parameters	5650/0/475	7299/12/475	8804/0/472	6774/0/472
R_1, observed reflections	0.0499	0.0451	0.0632	0.0614

dx.doi.org/10.1021/ic2012414 | *Inorg. Chem.* 2012, 51, 3366−3373

concentrated to about 10 mL under reduced pressure, and hexanes (ca. 5 mL), was added. The mixture was heated to optical clarity and cooled to about −18 °C for 2 d to give **3** as purple blocks. Yield 0.264 g (17%), mp 205 °C. Anal. Calcd. for **3**: C, 80.53; H, 7.32; N, 3.91. Found: C, 80.81; H, 7.86; H, 3.64. UV−vis, nm (ε, M^{-1} cm^{-1}) 526 (br) (15000). IR, cm^{-1}: 3480, 3380, 3360 ν(N−H), 385 ν(Co−N).

Ni{N(H)Ar^{Me_6}}$_2$ (4). To a solution of $Ar^{Me_6}NH_2$ (0.736 g, 2.2 mmol) in about 40 mL of Et_2O was added LiBu^n (2.5 M in C_6H_{14}) (0.97 mL, 2.4 mmol) at 0 °C. After 2 h, the solution was added dropwise to a stirred suspension of $NiBr_2$(DME) (0.242 g, 1.1 mmol) in Et_2O (ca. 25 mL) at about 0 °C. A dark blue color resulted immediately. After stirring at ambient temperature overnight, the solvent was removed under reduced pressure. Hexane (ca. 50 mL) was added, and the mixture was stirred briefly, after which it was filtered over Celite and washed with hexane (ca. 30 mL). The solution was concentrated under reduced pressure to incipient crystallization (ca. 20 mL). Storage at about −18 °C for 4 d afforded small blue, needle-shaped crystals of **4**. Yield 0.326 g (41%), mp 195 °C. Anal. Calcd. for 4: C, 80.56; H, 7.33; N, 3.92. Found: C, 80.91; H, 7.41; N, 3.78. UV−vis, nm (ε, M^{-1} cm^{-1}) 726(s,br) (5530). IR, cm^{-1}: 3480, 3380, 3360 ν(N−H), 385 ν(Ni−N).

X-ray Crystallography. Crystals of appropriate quality for X-ray diffraction studies were removed from the Schlenk tube under a stream of nitrogen and immediately covered with a thin layer of hydrocarbon oil (Paratone-N). A suitable crystal was selected and attached to a glass fiber and quickly placed in a low-temperature stream of nitrogen (ca. 90 K).[11] Data for compounds **1**−**4** were obtained on a either a Bruker SMART 1000 or SMART APEX instrument using Mo K_α radiation (λ = 0.71073 Å) in conjunction with a CCD detector. The collected reflections were corrected for Lorentz and polarization effects and for absorption by use of Blessing's method as incorporated into the program SADABS.[12] The structures were solved by direct methods and refined with the SHELXTL v.6.1 software package.[13] Refinement was by full-matrix least-squares procedures with all carbon-bound hydrogen atoms included in calculated positions and treated as riding atoms. N-bound hydrogens were located directly from the Fourier difference map. A summary of crystallographic and data collection parameters for **1**−**4** is given in Table 1.

Magnetic Measurements. Direct current (DC) magnetization measurements *M* vs *T* and *M* vs *H* at constant *T* for the nickel samples were obtained at Northeastern University using a Quantum Design MPMS SQUID magnetometer in applied fields up to 5 T on about 20−30 mg samples in Quantum Design Delrin holders sealed under nitrogen with Apiezon-N grease. Similar measurements were performed at U. C. Davis on the cobalt complexes also using a Quantum Designs MPMS SQUID magnetometer in applied fields up to 7 T on about 5−10 mg samples sealed in quartz tubes under vacuum. Three consecutive measurements were taken at each temperature or field. The spread in μ_{eff} values near ambient temperature were generally ≤0.05 Bohr Magnetons; all magnetic measurements were corrected using Pascal's constants.[14]

RESULTS AND DISCUSSION

Synthesis. Compounds **1**−**4** were synthesized by simple salt elimination routes shown in Scheme 1. A typical procedure entailed slow addition of an ether solution of freshly prepared lithium primary aryl amide Li{N(H)Ar} to an ether suspension of the metal(II) halide or metal halide-ether complex that was cooled to about 0 °C. The initial pale color of the reaction mixtures deepened upon slow warming to room temperature. Continued stirring for *ca.* 12−24 h followed by workup, afforded crystals of **1**−**4**, which were grown from filtered hexane or toluene extracts of the crude product.

Scheme 1. Synthetic Routes to 1−4

$$2\ Li\{N(H)Ar\} + CoCl_2 \xrightarrow{Et_2O} Co\{N(H)Ar\}_2 + 2\ LiCl$$

$$2\ Li\{N(H)Ar\} + NiBr_2(DME) \xrightarrow{Et_2O} Ni\{N(H)Ar\}_2 + 2\ LiBr$$

Ar = C_6H_3-2,6(C_6H_2-2,4,6-Pr^i_3)$_2$, $Ar^{Pr^i_6}$, **1** (Co) and **2** (Ni)
Ar = C_6H_3-2,6(C_6H_2-2,4,6-Me^i_3)$_2$, Ar^{Me_6}, **3** (Co) and **4** (Ni)

The synthesis of **1**−**4** differs from the approach used for the iron complexes Fe{N(H)$Ar^{Pr^i_6}$}$_2$ and Fe{N(H)Ar^{Me_6}}$_2$ which were obtained by treatment of Fe{N($SiMe_3$)$_2$}$_2$[15] with 2 equiv of the respective primary amines.[5] This approach was used when the alkali metal salt elimination route employed here proved unsatisfactory owing to long reaction times and the formation of anionic metal salts. In contrast, the greater solubility of $CoCl_2$ in ether permitted relatively rapid reactions to afford **1** and **3** in acceptable yields. For the nickel amides the more soluble $NiBr_2$(DME) complex[10] was employed to obtain **2** and **4**.

Structures. The structures of **1** and **2** are illustrated in Figures 2 and 3, and some important bond lengths and angles are presented in Table 2 which also includes data for their manganese[16] and iron[5] congeners. They are characterized by crystallographically required centers of symmetry at the metals that yield strictly linear N−M−N moieties. The *ipso* carbons of

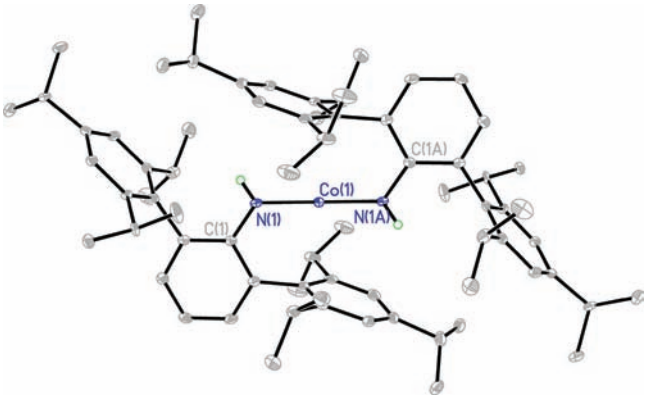

Figure 2. Thermal ellipsoid (50%) drawing of the linear coordinated bisamido cobalt Co{N(H)$Ar^{Pr^i_6}$}$_2$ (**1**). Hydrogen atoms (except N−H) are not shown. Co(1)−N(1,1A) 1.8645(19) Å ; Co(1)---(*ipso*-Mes C) 2.61 Å (avg.); N(1)−Co(1)−N(1A) 180.0°. Symmetry transformations used to generate equivalent atoms: −*x*+2,−*y*+2,−*z*.

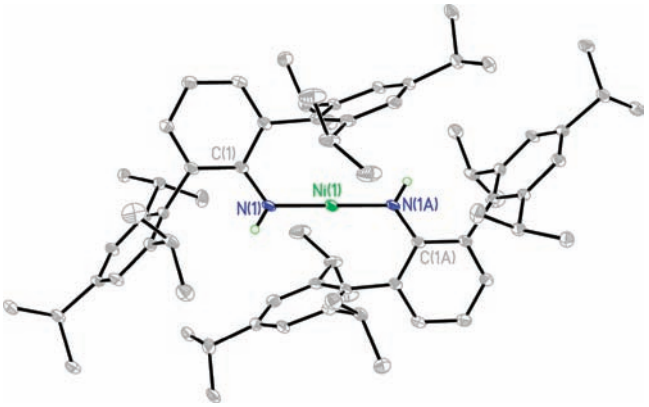

Figure 3. Thermal ellipsoid (50%) drawing of the linear bisamido nickel Ni{N(H)$Ar^{Pr^i_6}$}$_2$ (**2**). Hydrogen atoms (except N−H) are not shown. Ni(1)−N(1,1A) 1.8284(15) Å ; Ni(1)---(*ipso*-Mes C) 2.58 Å (avg.) ; N(1)−Ni(1)−N(1A) 180.0°. Symmetry transformations used to generate equivalent atoms: −*x*+2,−*y*+2,−*z*.

dx.doi.org/10.1021/ic2012414 | *Inorg. Chem.* 2012, 51, 3366−3373

the central aryl rings of the terphenyl group, the two nitrogens, hydrogens, and each metal, form a planar array with the

Table 2. Selected Interatomic Distances (Å) and Angles (deg) for the Linear Complexes 1 and 2, and the Analogous Mn[16] and Fe[5] Derivatives

	Mn{N(H)Ar$^{Pr^i_6}$}$_2$	Fe{N(H)Ar$^{Pr^i_6}$}$_2$	Co{N(H)Ar$^{Pr^i_6}$}$_2$ (**1**)	Ni{N(H)Ar$^{Pr^i_6}$}$_2$ (**2**)
M–N (Å)	1.952(2)	1.907(14)	1.8645(19)	1.8284(15)
M---(C7,7A) (Å)	2.73	2.79	2.61	2.58
N–M–N (deg)	176.09(12)	180.0	180.0	180.0
M–N–H (deg)		117.5(16)	121(2)	119.0(15)
C–N–M (deg)		130.06(11)	126.20(15)	126.24(11)

terphenyls disposed in a trans-fashion to afford local C_{2h} symmetry for the M{N(H)C(*ipso*)}$_2$ cores. The M–N bond length decreases slightly between cobalt and nickel consistent with the decreasing size of the metal radius on proceeding to the right across the d-element series.[17] The bond lengths are also significantly shorter than the 1.907(14) and 1.952(2) Å observed in the corresponding iron[5] and manganese[16] complexes. There are also relatively close approaches (2.61 Å, Co; 2.58 Å, Ni) between the metal and *ipso*-carbon of one of the flanking aryl rings of the terphenyl ligand.

The structure of **1** features the first example of linear coordination for a homoleptic amido cobalt species in the solid state. In the gas phase Co{N(SiMe$_3$)$_2$}$_2$ (Co–N = 1.84(2) Å)[15] was shown to have linear coordination by electron diffraction although this molecule associates through N(SiMe$_3$)$_2$ bridging in the solid state to yield a dimeric species with three coordinate cobalts.[18] Linear, or near linear (≥175° interligand angle), geometry in the solid state is quite rare for two coordinate cobalt complexes and is precedented by the almost linear thiolato derivative Co(SAr$^{Pr^i_6}$)$_2$[19] (S–Co–S = 179.52(2) Å) and the heteroleptic complex Co(Ar$^{Pr^i_4}$){N(SiMe$_3$)$_2$}[20] (C–Co–N = 179.02(11); Ar$^{Pr^i_4}$ = C$_6$H$_3$-2,6(C$_6$H$_3$-2,6-Pr$^i_2$)$_2$). The cobalt diaryl Co(Ar^{Me_6})$_2$ (C–Co–C = 172.17(11)°) is the only other two-coordinate cobalt species whose interligand angle exceeds 170°.[21] The Co–N distance in **1** (1.8645(14) Å) is similar to the 1.84(2) Å reported for Co{N(SiMe$_3$)$_2$}$_2$[15] in the vapor phase and the 1.8747(14) Å for Co(Ar$^{Pr^i_4}$){N(SiMe$_3$)$_2$} in the solid.[20] However, it is noticeably shorter than the Co–N distances in the bent geometry, two-coordinate complexes Co{N(SiMePh$_2$)$_2$}$_2$ (Co–N = 1.901(3) Å, N–Co–N = 147.0(1)°),[22] Co{N(Ph)BMes$_2$}$_2$ (Co–N = 1.909(5) Å, N–Co–N = 127.1(2)°)[23] and in Co{N(Mes)BMes$_2$}$_2$ (Co–N = 1.910(3) Å, N–Co–N = 168.4(1)°).[24] These structural data are in harmony with the view that terphenyl based ligands differ from other sterically demanding substituents because they protect space primarily via the shielding action of their flanking aryl rings whereas most sterically crowded ligands offer steric protection by occupying the space adjacent to the protected center. Seemingly, the close-in steric effects in the latter cases can more readily produce lengthened bonds than the shielding action of terphenyl ligands.

The nickel derivative **2** has a structure very similar to that of **1** and also to that of the recently reported two coordinate linear N–Ni–N species Ni{N(H)Ar$^{Pr^i_4}$}$_2$ (Ni–N = 1.818(3) Å) reported by Cui and co-workers.[24] This distance and that in **2** (1.8284(15) Å) are almost identical. As in the case of **1** the Ni–N bond lengths in the sterically crowded, bent, two-coordinate Ni{N(Ph)BMes$_2$}$_2$ (Ni–N = 1.885(4) Å, N–Ni–N = 135.7(1)°)[25] and Ni{N(Mes)BMes$_2$}$_2$ (Ni–N = 1.866(2) Å avg)[23] are longer. A much shorter bond length of 1.663(3) Å has been observed recently in the multiple bonded, two-coordinate Ni(II)-imido carbene complex [{CHN(C$_6$H$_3$-2,6-Pr$^i_2$)}$_2$C]-NiNAr^{Me_6}.[26]

The structures of Co{N(H)Ar^{Me_6}}$_2$ (**3**, Figure 4) and Ni{N(H)Ar^{Me_6}}$_2$ (**4**, Figure 5) are characterized by significant bending of the N–M–N core array as shown in Table 3. The M–N bond lengths display the same trend as the compounds listed in Table 2 with very similar M–N and M--C distances being apparent. The smaller terphenyl substituents permit N–

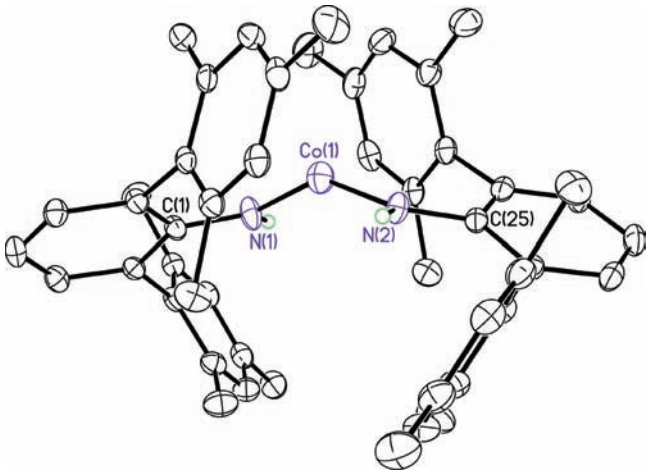

Figure 4. Thermal ellipsoid (50%) drawing of the bent geometry bisamido cobalt derivative Co{N(H)Ar^{Me_6}}$_2$ (**3**). Hydrogen atoms (except N–H) are not shown. Co(1)–N(1,2) 1.845(8), 1.827(8) Å ; Co(1)---(*ipso*-C) 2.56 Å (avg.); N(1)–Co(1)–N(2) 144.1(4)°.

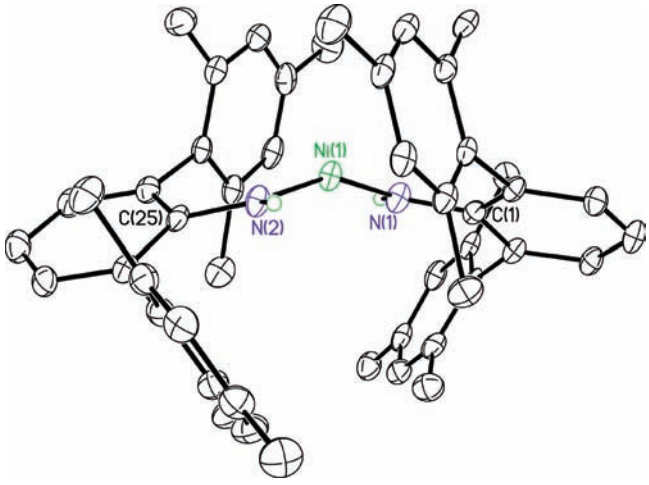

Figure 5. Thermal ellipsoid (50%) drawing of the bent bisamido nickel Ni{N(H)Ar^{Me_6}}$_2$ (**4**). Hydrogen atoms (except N–H) are not shown. Ni(1)–N(1,2) 1.819(3), 1.812(3) Å; Ni(1)---(*ipso*-Mes C) 2.56 Å (avg.) ; N(1)–Ni(1)–N(2) 154.60(14)°.

M–N angles of 144.1(4)° in **3** and 154.60(14)° in **4**. These angles are wider than the 141.19(9) and 138.19(9)° observed in the iron and manganese congeners possibly as a result of the increase in the effective steric crowding arising from the smaller size of the cobalt and nickel atoms.[17]

dx.doi.org/10.1021/ic2012414 | *Inorg. Chem.* 2012, 51, 3366–3373

Table 3. Selected Interatomic Distances (Å) and Angles (deg) for the Bent Complexes 3 and 4 for the Analogous Mn[16] and Fe[5] Derivatives

	$Mn\{N(H)Ar^{Me_6}\}_2$[15]	$Fe\{N(H)Ar^{Me_6}\}_2$[5]	$Co\{N(H)Ar^{Me_6}\}_2$ (3)	$Ni\{N(H)Ar^{Me_6}\}_2$ (4)
M−N(1)	1.976(2)	1.909(3)	1.827(8)	1.819(3)
M−N(2)	1.982(3)	1.913(3)	1.845(8)	1.812(3)
M---(C)[a]	2.63	2.64	2.56	2.56
N(1)−M−N(2)	138.19(9)	141.94(16)	144.1(4)	154.60(14)
M−N(1)−H(1)		116	116.7	117.8
M−N(2)−H(2)		114	118.6	117.8
C(1)−N(1)−(M)		128.5(3)	126.6(7)	124.3(3)
C(25)−N(2)−(M)		127.2(3)	122.9(7)	124.3(3)

[a]The average distance of two M---(*ipso*-C (flanking ring)) approaches is given.

Electronic Spectroscopy. For a free ion Co^{2+} the ground state is $^4F_{9/2}$ which in a linear crystal field (assuming $D_{\infty h}$ symmetry) splits into $^4\Sigma_g^+$, $^4\Pi_g$, $^4\Delta_g$, $^4\Phi_g$ component states of which $^4\Sigma_g^+$ lies lowest. For a free ion Ni^{2+} the ground state is $^3F_4$ and the ordering of the component states is expected to be the inverse of those of cobalt. In each case at least three bands are expected with the possibility of further bands from transition to the ^4P (split into $^4\Sigma_g$ and $^4\Pi_g$) state. Clearly the spectra of **1**−**4** display no such complexity. Only one absorption is observed in the spectra of the nickel complexes **2** and **4** in the red region of the spectrum at 770 and 726 nm. This is consistent with the blue color of the complexes reported. Similarly only a single band at 526 nm is observed in the spectrum of the cobalt species **3** although two bands at 364 and 506 nm were observed for **1**. At present, it is not possible to make an assignment of these bands. It is a possibility that the splittings of the F ground states are small and the transitions lie in the near-infrared outside of the wavelength range 250−1100 nm of the spectrometer. In this case the two bands observed may be a result of transitions to the split excited P state. However, the intensity of the absorptions suggests that they could be due to charge transfer to the metals from the amido ligands. Full molecule, density functional theory (DFT) calculations on a series of amido complexes will be required to shed further light on their electronic spectra.

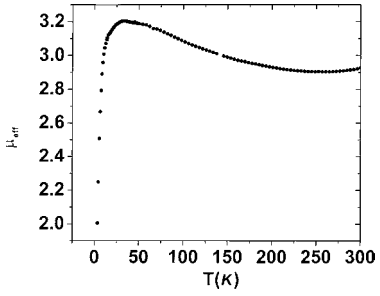

Figure 6. μ_{eff} vs T plot for the linear nickel complex **2**, at H(DC) = 1000 Oe.

DC Magnetometry Measurements. Figures 6 and 7 show plots of the effective moments derived from DC magnetization vs T for the linear (**2**) and bent (**4**) nickel(II) complexes (ca. 30 mg of polycrystalline samples in sealed holders under dry N_2). Consistent with the results reported for the analogous pair of iron complexes, the linear derivative **2** clearly shows a higher moment reaching a maximum μ_{eff} of about 3.20 Bohr Magnetons around 35−40 K (Figure 6) with a value of 2.92 μ_B at ambient temperature. This value is similar to the 2.79 μ_B

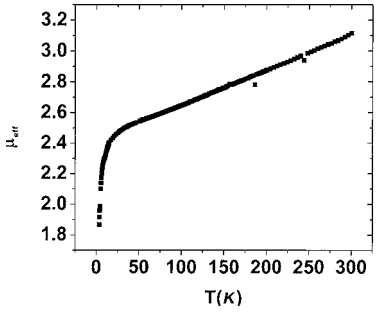

Figure 7. μ_{eff} vs T plot for the bent nickel complex **4**, at H(DC) = 1000 Oe.

reported for the related linear $Ni\{N(H)Ar^{Pr^i_4}\}_2$ derivative,[24] whose Ar^{Pri}_4 substituents on N differ only by the absence of the two Pr^i groups that are present in the para positions of the flanking aryls (C_6H_2-2,4,6-Pr^i_3) of the $Ar^{Pr^i_6}$ substituent in compound **2**. The bent Ni complex **4** behaves very differently in an applied field of 1000 Oe from its linear counterpart, showing a steady, monotonic decrease in μ_{eff} to ∼25K at which temperature a sharp change in slope reflecting significant single ion zero field splitting (Figure 7). In fact, the overall temperature profiles of μ vs T for **2** and **4** are somewhat reminiscent of those found by Figgis and co-workers[27] for classic six coordinate Fe^{2+} species perturbed via a large local low-symmetry ligand field components, for example, C_{2v} and varying degrees of electron delocalization. The d_{xz}, d_{yz} degeneracy of Figure 1, absent Jahn−Teller distortion, clearly presents the possibility of a strong first order orbital angular momentum contribution to the moment for the rigorously linear nickel complex **2**. Apparently this does not occur as the limiting value of the moment should then be about 5.6 μ_B[28] and not slightly greater than 3.0 μ_B. Similar magnetic moments have been observed for all of the other rigorously linear two coordinate Ni(II) complexes with which we are familiar in the literature and for which detailed[24,26] or otherwise[17,19,23] magnetometry studies exist. It seems likely that π bonding effects involving the d_{xz} d_{yz} pair lift their degeneracy. This idea can and will be tested via synthesis and detailed investigation of the presumably linear putative $Ni\{C(SiMe_3)_3\}_2$ or other linear two coordinate Ni(II) complexes with sigma bonding only ligands. At present, unfortunately, no stable two-coordinate linear geometry Ni(II) complex with exclusively σ-bonding ligands is known.

Finally, we point to Figures 8 and 9 below which show the isothermal magnetization, M vs H, of **2** and **4**, respectively, at ∼3.5 K. In view of their magnetizations at 5 T, it is evident that these systems are relatively far from magnetic saturation where M_{Sat} (spin only) = 11,165 emu/mol for S = 1 suggesting

dx.doi.org/10.1021/ic2012414 | Inorg. Chem. 2012, 51, 3366−3373

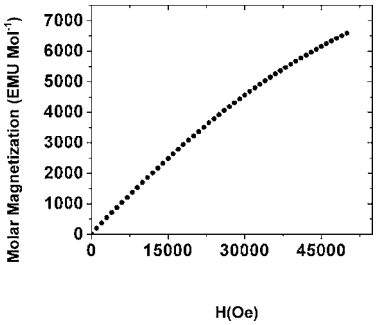

Figure 8. Isothermal magnetization plot for the linear coordinated Ni^{2+} amido complex **2** at 3.5 K.

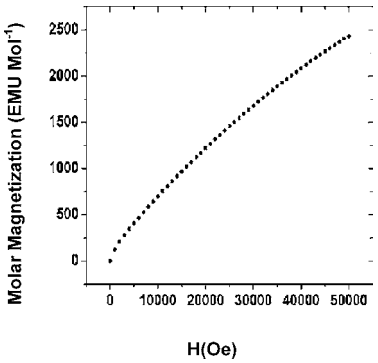

Figure 9. Isothermal magnetization plot for the bent geometry Ni^{2+} amido complex **4** at 3.5 K.

substantial (~20 cm^{-1} or greater) and likely positive zero field splittings where D values of this order are not uncommon for non-Kramers ions such $S = 1$ Ni^{2+}.[30]

We now turn to the magnetic studies of the cobalt complexes **1** and **3**. Unlike the nickel complexes **2** and **4**, both **1** and **3** possess magnetic moments that are significantly greater than the spin only values as a result of spin orbit coupling effects. However, the expected significant orbital angular momentum quenching effects arising from the bent (local C_{2v}) chromophore of cobalt complex **3** are apparent in Figures 10 and 11

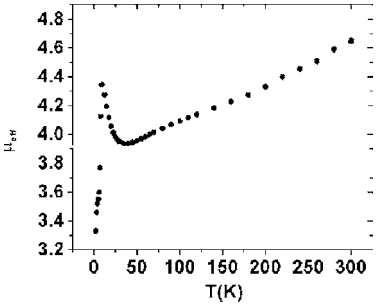

Figure 10. Plot of μ_{eff} vs T for the bent geometry Co^{2+} amide **3** at H(DC) = 100 Oe.

below wherein μ_{eff} for **3** is seen to exhibit a marked decrease in magnitude over the entire temperature range relative to **1** (Figure 12 and 13). Nevertheless μ_{eff} is measurably enhanced by spin−orbit coupling interactions for $T >$ about 50K. The sharp and unexpected change in the μ_{eff} observed at about 25 K in Figure 10 may be due to a spin-state crossover

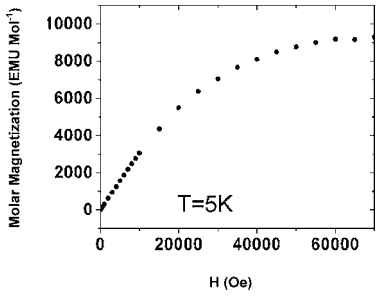

Figure 11. Isothermal magnetization plot for the bent geometry Co^{2+} amide **3** at 5 K out to 7 T.

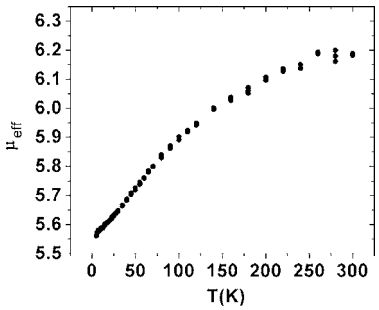

Figure 12. μ vs T for the linear coordinated Co^{2+} complex **1** at H(DC) = 100 Oe.

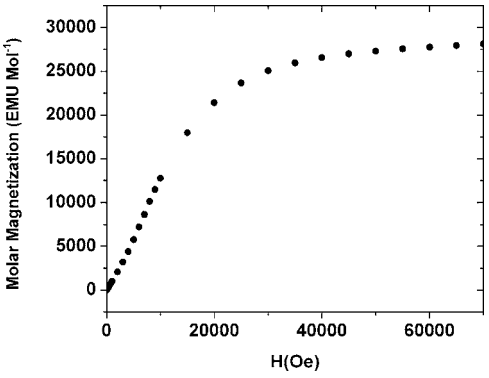

Figure 13. Isothermal magnetization of the linear coordinated Co^{2+} complex **1** at 5 K out to 7 T.

associated with a structural phase transformation. Definitive confirmation of this possibility must await either magnetic hysteresis, heat capacity, or lower temperature structure investigations. In any event, this phenomenon has been recently observed in a related two-coordinate aryl cobalt(II) amido species.[29]

The SQUID magnetometry results for the linear cobalt(II) complex **1** are shown in Figures 12 and 13. Recall that from Figure 1 the high-spin d^7 configuration of Co(II) indicates that **1** corresponds to an orbitally nondegenerate spin-quartet ground state and as such cannot exhibit direct first order (orbital) enhancement of its ground state magnetic moment. Nevertheless, its ambient temperature moment (ca. 6.2 μ_B exceeds the spin-only value (3.87 μ_B) by well over 2 Bohr Magnetons. Enhanced magnetic moments are fairly typical of spin−orbit coupling interactions for Co(II) (earlier investigations of this phenomenon for tetrahedral Co^{2+} complexes confirmed orbital contributions ranging to 1.1 μ_B[31]). However in the specific case of **1** it is extremely large especially in the

dx.doi.org/10.1021/ic2012414 | Inorg. Chem. 2012, 51, 3366−3373

context of a free-ion value of the moment of 6.63 μ_B. Other near linear two-coordinate cobalt(II) complexes, Co(Ar$^{Pr^i_4}$)-{N(SiMe$_3$)$_2$} (C−Co−N = 179.02(1)°, μ_B = 5.82 μ_B)[20] and Co(SAr$^{Pr^i_6}$)$_2$ (S−Co−S = 179.52(2)°, μ_B = 5.75),[19] also exhibit unusually high magnetic moments. The slightly lower value of the moment for Co(Ar$^{Pr^i_4}$){N(SiMe$_3$)$_2$}[20] vs **1** likely owes to its heteroleptic nature as well as slight bending, perhaps testifying to the extraordinary sensitivity of the orbital contributions to details of local symmetry. In a very real sense we are broaching free ion magnetic behavior Co(II) in **1** through the agency of very strong spin−orbit and near maximum coordination unsaturation. In the symmetry of rigorously linear homoleptic two coordination, one expects less excited state splitting and somewhat more enhancement of spin−orbit coupling effects. In addition with an overall smaller total ligand field splitting effect (10Dq linear) from the presence of only two ligands, spin−orbit coupling effects should likewise be maximized. This statement is best understood with use of the equation $\mu_{eff} = \mu_{S0}(1 - \alpha\cdot\lambda/10Dq)$ (ignoring any temperature independent paramagnetism).[28] For Co^{2+}, λ is −172 cm^{-1}, for an F ground state, α = 4 and therefore $\alpha\cdot\lambda$ = −688 cm^{-1}. In addition, for a two-coordinate ligand field 10D$_q$ must be relatively small and may be roughly one-half of a tetrahedral field. In other words, the correction for the linear field is expected to be substantially larger than that for a tetrahedral field. Since tetrahedral fields are already known to produce enhancements of the magnetic moment by over 1 μ_B for Co^{2+} complexes,[31] a correction of 2 μ_B or more seems reasonable for a linear two-coordinate complex. Furthermore, electron paramagnetic resonance (EPR) spectra for **1** and **3** afford g values of 6−6.7 g with a hyperfine (^{59}Co(I = 7/2)) coupling constant near 1 GHz (See Supporting Information) at 5 K consistent with substantial spin−orbit coupling. No EPR signals could be detected for the nickel species **2** and **4**. More extensive EPR studies of **1**−**4** are in hand. Finally it is worthwhile to direct the reader to the magnetization results in Figure 13. These confirm near saturation for **1** at 7 T. The spin−orbit coupling effects for the linear complex **1** are indeed equivalent to adding two full spins to the S = 3/2 d^7 configuration of Co(II) leading to an effective moment reminiscent of that of high−spin (S = 5/2) Fe(III).

SUMMARY

The use of two electronically similar but sterically different ligands has allowed the linear and bent geometry pairs of amido complexes of Co^{2+} and Ni^{2+} to be characterized and their magnetic properties to be studied. For the linear nickel, d^8 species **2**, where a first order orbital angular momentum is predicted (cf. Figure 1), essentially no enhancement of the magnetic moment above its spin only value is observed. This may be a result of metal−ligand π-bonding which lifts the degeneracy of the potentially π-bonding d$_{xz}$ and d$_{yz}$ orbitals which quenches the orbital moment. The bent geometry nickel species **2** also afforded a magnetic moment close to the spin only value. For the d^7 cobalt amido complexes **1** and **3**, no first order orbital angular momentum is predicted, yet magnetic moments well above the predicted spin only values are observed for both species. For linear geometry species **1** a μ_{eff} value that is more than 90% of the free ion value is observed at ambient temperature. This unusual result is due to the rigorously linear coordination and weak ligand field in addition to the dominant spin−orbit coupling interactions.

ASSOCIATED CONTENT

Supporting Information

CIF files for the X-ray structures of **1**−**4**. EPR Spectra of **1** and **3**. UV−vis spectra of **1**−**4**. This material is available free of charge via the Internet at http://pubs.acs.org.

AUTHOR INFORMATION

Corresponding Author

*E-mail: pppower@ucdavis.edu.

Notes

The authors declare no competing financial interest.

ACKNOWLEDGMENTS

We are grateful to the National Science Foundation (CHE-0948417) for financial support A.M.B thanks the National Science Foundation for a graduate student fellowship.

REFERENCES

(1) (a) Power, P. P. *Inorg. Chem.* **1989**, *8*, 177. (b) Power, P. P. *Chemtracts* **1994**, *6*, 181.
(2) Kays, D. L. *Dalton Trans.* **2011**, *40*, 769.
(3) (a) Reiff, W. M.; La Pointe, A. M.; Witten, E. H. *J. Am. Chem. Soc.* **2004**, *126*, 10206. The Fe{C(SiMe$_3$)$_3$}$_2$ studied in (a) was originally described in: (b) Viefhaus, T.; Schwartz, W.; Hübler, K.; Locke, K.; Weidlein, J. *Z. Anorg. Allg. Chem.* **2001**, *627*, 715. (c) LaPointe, A. M. *Inorg. Chim. Acta* **2003**, *345*, 359.
(4) Reiff, W. M.; Schulz, C. E.; Whangbo, M. H.; Seo, J. I.; Lee, Y. S.; Potratz, G. R.; Spicer, C. W.; Girolami, G. S. *J. Am. Chem. Soc.* **2009**, *131*, 404.
(5) Merrill, W. A.; Stich, T. A.; Brynda, M.; Yeagle, G. J.; De Hont, R.; Fettinger, J. C.; Reiff, W. M.; Schulz, C. E.; Britt, R. D.; Power, P. P. *J. Am. Chem. Soc.* **2009**, *131*, 12693.
(6) Krishnamurthy, R.; Schaap, W. B. *J. Chem. Educ.* **1969**, *46*, 799.
(7) Pangborn, A. B.; Giardello, M. A.; Grubbs, R. H.; Rosen, R. K.; Timmens, F. J. *Organometallics* **1996**, *15*, 518.
(8) Tilley, T. D.; Gavenonis, J. *Organometallics* **2000**, *21*, 5549.
(9) Twamley, B.; Hwang, C.-S.; Hardman, N. J.; Power, P. P. *J. Organomet. Chem.* **2000**, *609*, 152.
(10) Casalnuovo, A. L.; Rajan Babu, T. V.; Ayers, T. A.; Warren, T. H. *J. Am. Chem. Soc.* **1994**, *116*, 9869.
(11) Hope, H. *Prog. Inorg. Chem.* **1995**, *41*, 1.
(12) (a) Blessing, R. H. *Acta Crystallogr.* **1995**, *A51*, 33. (b) Sheldrick, G. M. *SADABS, Siemens Area Detector Absorption Correction*; Universität Göttingen: Göttingen, Germany, 2008.
(13) (a) Sheldrick, G. M. *SHELXTL*, Version 6.1; Bruker AXS Inc.: Madison, WI, 2002. (b) Sheldrick, G. M. *SHELXS97 and SHELXL97*; Universität Göttingen: Göttingen, Germany, 1997.
(14) Bain, G. A.; Berry, J. F. *J. Chem. Educ.* **2008**, *85*, 532.
(15) Andersen, R. A.; Faegri, K.; Green, J. C.; Haaland, A.; Lappert, M. F.; Leung, W.-P.; Rypdal. *Inorg. Chem.* **1988**, *27*, 1782.
(16) Ni, C.; Rekken, B.; Fettinger, J. C.; Long, G. J.; Power, P. P. *Dalton Trans.* **2009**, 8349.
(17) Pauling, L. *J. Am. Chem. Soc.* **1947**, *69*, 542.
(18) Murray, B. D.; Power, P. P. *Inorg. Chem.* **1984**, *23*, 4584.
(19) Nguyen, T.; Panda, A.; Olmstead, M. M.; Richards, A. F.; Stender, M.; Brynda, M.; Power, P. P. *J. Am. Chem. Soc.* **2005**, *127*, 8545.
(20) Ni, C.; Stich, T. A.; Long, G. J.; Power, P. P. *Chem. Commun.* **2010**, 4466.
(21) Kays, D. L.; Cowley, A. R. *Chem. Commun.* **2007**, 1053.
(22) Bartlett, R. A.; Power, P. P. *J. Am. Chem. Soc.* **1987**, *109*, 7563.
(23) Chen, H.; Bartlett, R. A.; Olmstead, M. M.; Power, P. P.; Shoner, S. C. *J. Am. Chem. Soc.* **1990**, *112*, 1048.
(24) Li, J.; Song, H.; Cui, C.; Cheng, J.-P. *Inorg. Chem.* **2008**, *47*, 3468.

(25) Bartlett, R. A.; Chen, H.; Power, P. P. *Angew. Chem., Int. Ed. Engl.* **1989**, *28*, 316.
(26) Laskowski, C. A.; Miller, A. J. M.; Hillhouse, G. L.; Cundari, T. R. *J. Am. Chem. Soc.* **2011**, *133*, 771.
(27) Figgis, B. N.; Lewis, J.; Mabbs, F. E.; Webb, G. A. *J. Chem. Soc. (A)* **1967**, 442.
(28) Drago, R. S. *Physical Methods in Chemistry*; Saunders: Philadelphia, PA, 1992; p 484.
(29) Ni, C.; Fettinger, J. C.; Long, G. J.; Power, P. P. *Inorg. Chem.* **2009**, *48*, 2443.
(30) Boca, R. *Coord. Chem. Rev.* **2004**, *248*, 757.
(31) Holm, R. H.; Cotton, F. A. *J. Chem. Phys.* **1959**, *31*, 788.